J. Chem. Soc. Nigeria, Vol. 47, No. 5, pp 1075 - 1098 [2022]

ANTI-CORROSIVE POTENTIALS OF NAPHTHO-QUINONE/NAPHTHA-ALDEHYDE SCHIFF BASES FOR MILD STEEL IN HCL MEDIUM: SYNTHESIS, CHARACTERIZATION AND DFT STUDIES

T. C. Wodi [a,b], C. Festus[a,]* and E. Nlemonwu[a] ,

[a]Department of Chemistry, Ignatius Ajuru University of Education, Rivers State, Nigeria
[b]Community Boys Senior Secondary, Elelenwo, Port Harcourt, Rivers State, Nigeria.
***e-mail:chidebestokwu80@gmail.com**

ABSTRACT

The corrosion inhibition of four ligands; L1, L2, L3 and L4 synthesized through reflux condensation, and characterized via spectroscopic methods were examined using weight loss measurements and Density Functional Theory(DFT). Factors like ligand's chemical structure, immersion time, concentration, and temperature which affect efficiency of corrosion inhibition were evaluated. The experimental results revealed declined weight losses from 0.02-0.004g, 0.06-0.00625g and 0.11450-0.06938g at 303K, 333K, and 363K temperature for concentration increase from 100-500ppm. The increase in weight loss arose from temperature (303-363K) increase. Obtained data denotes declined corrosion rate in the presence of the inhibitors in the acid solutions but decreased as the inhibition concentration increased at each temperature. The highest inhibition efficiency (%ηwL) for the ligands at 303K, 333K and 363K temperatures and 500 ppm concentration were observed as 89.39% (L3), 88.36% (L2) and 55.00% (L2) respectively. The exceptional inhibition proficiency of the ligands could be due to the availability of heteroatoms and aromatic rings with π-electrons within their structures. The increase in %ηwL for 5 hours immersion was in the order L2<L4<L1<L3, L1<L3<L4<L2 and L3<L1<L4<L2 at 303K, 333K, and 363K temperature respectively with L3 having the highest %ηwL at 89.39% at 303K. The desorption process of the ligands upon the mild steel surface (mss) followed Langmuir adsorption isotherm. The ΔG_{ads} values acquired were amid -18.1709 to -35.6765KJ mol^{-1} suggestive of adsorption of the studied inhibitors on mss been physisorption. Chemical calculations and molecular descriptors of dipole moment(μ), energy gap, *E*HOMO, and *E*LUMO were acquired via B3LYP level with 6-31G (d, p) basis, while global reactivity descriptors; global softness(S), global hardness(η), electrophilicity index(ω) were derive and analyze using Koopman's theorem. The ligands were found to be in good agreement with both experimental and theoretical results. The L3 ligand had the highest *E*HOMO value of - 8.4696567 denoting greater inhibition potency and conforming to the result obtained from corrosion %ηwL. The structural assemblages of the ligands were confirmed using spectroscopic and analytical methods.

Keywords: Synthesis, Ligands, Corrosion, Langmuir Isotherm, Density Functional Theory

INTRODCTION

Deterioration of a metal due to its environmental reaction is called corrosion, which occurs in the presence of oxygen and humidity [1]. The most practical and cost-effective available methods of corrosion safety remains the use of corrosion inhibitors [2]. By adsorbing on the surface, the latter inhibit the metal from corrosion, by creating a protective barrier between metal surfaces and electrolytes [3]. Physicochemical and electronic properties such as molecular size of an inhibitor, steric effects, type and electronic density of substituents within the inhibitor, inhibitor's orbital character, nature of metal and electrolytes are basic factors which influence the rate of adsorption of inhibitors on metallic surfaces [4]. In different acidic media of varied temperatures, countless inhibitor ligands have displayed good corrosion inhibition properties [5,6]. But organic compounds containing polar functional groups such as nitrogen, sulphur, and/or oxygen within a conjugated system, and hydrophobic moiety that will block the mss against the corrosive environment have been reported as effective corrosion inhibitors [7,8]. Though, the polar moieties in the organic inhibitors are considered to be responsible for forming the adsorption

ISSN 0795 - 22066

film [9]. Such compounds are often polymeric in nature with multiple active centres which facilitate complex formations [10]. The inhibitive power and effectiveness of polymeric corrosion inhibitors has been linked to their cyclic structural units, and the hetero atoms which serve as major adsorption centres [11]. Schiff bases are potential polymeric inhibitors owing to the presence of amine group [12], and electronegative heteroatoms [13,14]. The heterocyclic organic components of Schiff bases have been linked to their tendency in forming stronger coordination bonds and, as a result, increasing %^{n}wL based on the trend; oxygen<nitrogen<sulphur<phosphorus [15], and making them better inhibitors in acidic media [16]. Also, the surface state, and additional charge on the metal surface similarly influences the adsorption behaviour of inhibitors. With most known chemical corrosion inhibitors of metals and alloys been toxic, posing risks to human health and environment, the usage of polymeric organic inhibitors becomes more adequate [17]. For this reason, several researches have been targeted at the use of organic compounds as corrosion inhibitors [18,19,20] and this isn't an exception. The inhibition efficiencies of organic molecules depend on the adsorption abilities in addition to structural, mechanical, and chemical properties of the adsorption layer produced under a particular solution [9].

In order to support experimental studies, theoretical calculations are conducted to provide molecular level understanding of the observed experimental behaviour [21] of inhibitors. Among such, DFT has proven significant and appears more adequate for pointing out the changes in electronic structure responsible for inhibitory action [10]. The latter focuses more on the geometry of the inhibitor, and the nature f their molecular orbitals of the inhibitors [22].

MATERIALS AND METHODS

The solvents (ethanol,(C_2H_5OH), dimethyl-formamide($(CH_3)_2NCH$, dichloro-methane(CH_2Cl_2), dimethyl-sulphoxide($(CH_3)_2SO$ and chloroform($CHCl_3$) were acquired as drum standards. The reagents; 2-hydroxy-2,3-dihydronaphthalene-1,4-dione, 2-hydroxy-1-naphthaldehyde, 4-hydroxy-6-methylpyrimidin-2-amine 4-chloro-6-methylpyrimidin-2-amine, 2-amino-4-methylphenol, 3-chloro-5-(tri-fluoromethyl) pyridine were of A.R grade sourced from Sigma-Aldrich Coy. The studied inhibitor ligands (Fig. 1); L1, L2, L3 and L4 with molecular weights 281.262g/mol, 299.75g/mol, 279.278g/mol and 350.715g/mol respectively were synthesized following our earlier research methodologies [23,24]. The Bruker FT/IR-4100 Billerica spectrometer (4000–350 cm^{-1}) was utilized to acquire the vibrational spectral data as triplet scans with KBr disc method. The nuclear magnetic resonance (NMR) and electronic (UV-Vis) spectral analyses, as well as DFT evaluations were carried out following literature procedures [25,26,27]

ISSN 0795 - 22066

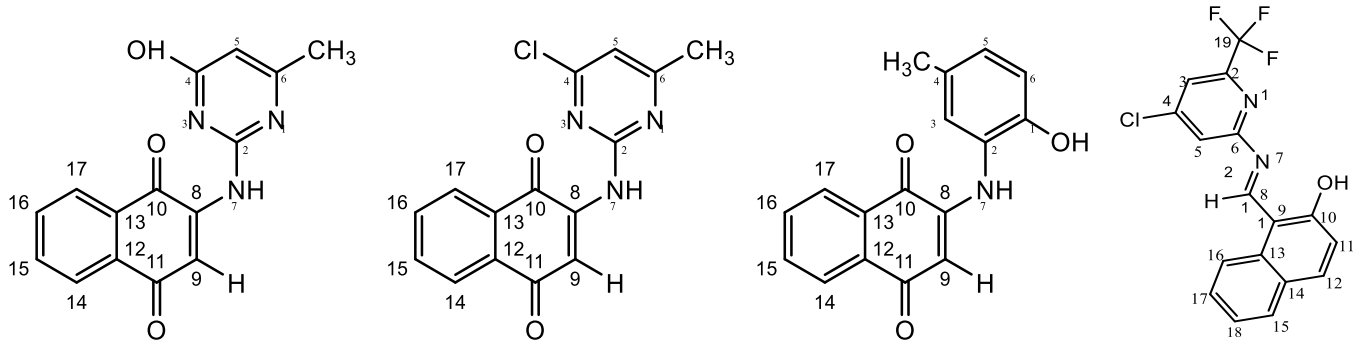

a b c d

Figure 1. Proposed Structures of (**a**) 2-((4-hydroxy-6-methylpyrimidin-2-yl)amino)naphthalene-1,4-dione(**L1**), (**b**) 2-((4-chloro-6-methylpyrimidin-2-yl)amino)naphthalene-1,4-dione(**L2**), (**c**) 2-((2-hydroxy-5-methylphenyl)amino)naph- thalene-1,4-dione(**L3**), and (**d**) (*E*)-1-(((4-chloro-6-(trifluoromethyl)pyridin-2-yl)imino)methyl)naphthalene-2-ol (**L4**)

Table 1. Analytical Data of the Synthesized Inhibitors

Ligands	Empirical Formula	Molecular Weight (g/mol)	Yield (%)	Elemental Data (%)					Melting Point (°C)
				C	H	N	Cl	F	
L1	$C_{15}H_{11}N_3O_3$	281.262	66.4	64.05 (63.96)	3.94 (4.02)	14.94 (15.00)	-	-	207-211
L2	$C_{15}H_{10}N_3O_2Cl$	299.756	63.7	60.09 (60.02)	3.36 (3.40)	14.02 (13.97)	11.82 (11.87)	-	248-251
L3	$C_{17}H_{13}NO_3$	279.278	71.8	73.10 (72.99)	4.69 (4.72)	5.01 (5.00)	-	-	231-234
L4	$C_{17}H_{10}N_2OF_3Cl$	350.715	59.6	58.21 (58.29)	2.87 (2.94)	7.99 (8.07)	10.22 (10.16)	16.25 (16.28)	219-222

Preparation of MS coupons

The ms sheets with thickness 0.5mm were purchased from Mile 3 market in Rivers State. The ms were cut into rectangular coupons of dimensions 40mm x 40mm. To obtain a very clean glossy surface, the coupons were carefully polished mechanically with emery paper, after which it was washed in distilled water (dist.-H_2O), degreased in ethanol, arid in acetone and stored in moisture free desiccators.

Gravimetric Measurements

Aggressive1M Hydrochloric acid solution was diluted with twofold dist.-H_2O. The solutions containing the ligands (Inhibitor solutions) with concentrations of 100, 300, and 500 ppm were adopted for the inhibition studies. These solutions were prepared via dissolution of 0.5g of the ligands in 50 mL in an organic solvent that is soluble with the ligands and made up to 1 dm^3 with 1M HCl. Blank solutions without the inhibitors were made with 100mL of 1M HCl as standard solutions. Similar beakers of 100 mL volume each were labelled 100ppm, 300ppm,

ISSN 0795 - 22066

500ppm and blank. These beakers were made to contain different concentrations of the ligands while the last beaker stands as blank. The ms coupons with 40mm x 4mm x 0.5mm size were abraded with emery paper and washed with dist.-H_2O, ethanol, and acetone, then arid for assessing. Time factor considered in this experiment for the immersion of the ms was 5 hours. The weights of the specimens were noted prior to immersion. After 5 hrs immersion, the specimens were removed from the acidic medium, polished, washed in double dist.-H_2O, degreased with ethanol, desiccated in CH_3COCH_3 and reassessed. All investigations were carried out twice. The corrosion rate (CR) computations were done with obtained mean weight loss values as follows [14]

$$CR = \Delta W/\Delta t \text{ ---------- (1)}$$

$$\Delta w = \frac{m1-m2}{A} \text{ ---------- (2)}$$

The percentage %ɳwL and surface coverage (Ɵ) were evaluated from CR values

$$\%_{ɳ}wL = CR_B - CR_1 / CR_B \times 100 \text{ ---------- (3)}$$

RESULTS AND DISCUSSIONS

Spectral Studies

The ^{1}HNMR spectra of the ligands (L1-L4) have been obtained (SM4-10). All the ligands exhibited peaks amid 7.79-6.56 ppm, 7.95-6.97 ppm, 8.00-7.99 ppm; and 8.19-10.77 ppm assignable to the aromatic protons of the naphthoquinone and naphthaldehyde groups separately. The higher peak values could be a consequence of the presence of highly electronegative fluorine atoms within the structure. The methyl substituents on L1, L2 and L3 ligands resonated at 2.48-2.49 ppm, while the peaks arising from the protons of the substituted pyrimidines, methyl-phenol and substituted pyridine molecules appeared at 6.06 ppm, 6.03 ppm, 6.06-6.56 ppm and 7.57-7.85 ppm respectively. The distinctive bands at 8.19 ppm, 4.46 ppm and 8.19 ppm within the hydrogen-NMR spectra of L1, L2 (SM4) and L3 (SM5) ligands were consistent of N–H moiety of a secondary amide, validating the proposed keto-imine structural assemblages. The latter suggests that Michael addition type of reaction occurred in which the carbon atom bearing the OH group within the naphthoquinone moiety was attacked in a nucleophilic fashion by the nitrogen atom of the amino group from the substituted pyrimidine and phenol moieties separately [28]. Contrarily, L4 ligand (SM6) presented a band at 12.0 ppm typical of HC=N moiety corroborating the formation of an enol-Schiff base. This conforms to comparable works on 2-hydroxy-1-naphthaldehyde-based Schiff bases where the ligand adopts enol-tautomeric assemblage [25,29]. The multiplet peaks in the ranges 7.33-7.80 ppm, 7.55-7.78 ppm, 7.55-8.18 ppm, as well as 8.56-9.49 ppm were apportioned to cyclic protons (H14-H16, and H14-17) for L1-L3 and L4 ligands respectively. The OH protons resonated at 9.19 (L1 and L3), and 14.51 (L4) ppm. The ^{13}C NMR spectra (SM7-10) of L1, L2, L3, and L4 ligands separately presented signals at 164.1(C10)-192.8(C11), 183.6(C10)-181.2(C11) ppm, 184.5(C10)-181.5(C11) ppm, and 108.3(C9) ppm consistent of carbonyl (C=O) carbon atoms [30]. The relatively low resonant frequency of the C=O group within L4 ligand is a consequence of the effect of the electronegative nitrogen and imine π-system. Peaks amid 112.4-138.4 ppm, 108.0-129.5 ppm, 76.63-134.4 ppm, and 118.7-141.4 ppm typical of aromatic carbon atoms of naphthalene and pyrimidine, phenol and pyridine groups. Additionally, the peaks arising from the carbon atoms of CH_3 appeared at 32.06, 23.44 ppm and 22.31 ppm respectively.

The infrared spectra of ligands (L1-L3) had strong absorption bands at 3316, 3397, and 3292 cm^{-1}; plus 1310, 1383 and 1365 cm^{-1} conforming to stretching, and bending vibrations of secondary amide groups; and C-N groups

ISSN 0795 - 22066

separately [28]. The N-H vibrations conforms to ketoimine structural assemblages for the L1-L3 ligands (Fig 1(a-c)). However, L4 ligand exhibited enol tautomer (Fig. 1d) with a band at 1627 cm^{-1} complimenting the observed C=NH peak at 12.0 ppm. The vibrations arising from the OH groups of the hydroxyl-substituted aromatic moieties were observed in the spectra of the ligands from 3416 cm^{-1} to 3651 cm^{-1} [31]. Very sharp to medium bands at 3176-3062 cm^{-1} and 3075-2918 cm^{-1} in the spectra of the ligands (L1-L3) were apportioned to cyclic (Ar-H) and methyl substituent/imine (CH_3/H-C=N) hydrogen stretching vibrations with corroborating C-H bending vibrations amid 1453 cm^{-1}, 1477 cm^{-1}, 1515 cm^{-1}, and 1474 cm^{-1} separately. The absorptions amid 1605-1659 cm^{-1}, 1592-1678 cm^{-1}, and 1615-1652 cm^{-1} are stretching bands of the ketonic C=O groups at C10 and C11 of the naphthoquinone moieties separately (Fig. 1(a-c)). The sharp bands at 1562-1594 cm^{-1} stood apportioned to stretching vibrations of the C=C groups within the ligand assemblages [23]. Additionally, the bands at 920-991cm-1 in the respective spectrum of the ligands conformed to *d*C–H vibrations, while the C-Cl and C-F bands of L2 and L4 ligands appeared at 749-874 cm^{-1}; and 834 cm^{-1}.

Corrosion Inhibition Studies

Gravimetric Quantities

Ligands' Effect on MS in Acid Corrosion Medium. The effect of ligands on ms was measured using gravimetric calculations in 1M hydrochloric acid with the ligands acting as the inhibitors at different concentrations and temperatures in a homogenous solution. The results obtained from total weight loss against concentration of the inhibitors are shown in Table 3. The result revealed that the inhibitors were absorbed, with a decline of weight loss as concentration increases. Figure 2(a, b and c) showed that as the concentration of the inhibitors decreases, the rate of corrosion increases. Whereas, the inhibition concentration increases with a decrease in CR at the same temperature and time (Table 3). Better corrosion inhibition behaviour was displayed by the ligands in disparity to corrosion of ms in a 1M hydrochloric acid solution. The coordination of the atoms of the ligands through the donor acceptors' interaction with the unshared pairs of electron attributes to the capability of the effective inhibition of the ligands towards ms [32].

Table 2. Spectral Data of the Synthesized Ligands

Spectral Analysis/Ligands		L1	L2	L3	L4
IR Spectral Data (cm^{-1})	OH	3651	3410	3485	3422
	NH	3316	3316	3292	-
	Ar. CH	3093	3176	3062	3106
	Ali.-CH_3	2969	3075	2918	-
	C=O	1659, 1605	1678, 1642	1680, 1615	-
	C=N	-	-	-	1627
	C=C	1562	1579	1594	1590
	C-N	1310	1383	1365	1322
	C-O	1255	1286	1295	1281
	C-C, n-ring	1201	1224	1238	1251

ISSN 0795 - 22066

	OH, bending	1042	1119	1045	1117
	C-H, cyclic bending	1453	1458	1515	1474
	d C-H, rocking in plane	974	982	991	920
	C-Cl	-	874	-	749
	C-F	-	-	-	834
NMR Data	**H[1]NMR**	2.48-2.49(*dd*, CH_3), 9.19(*s*, OH), 8.19(*m*, N-H),6.06 (H5), 6.56(s H9), 7.33–7.77(*dd*, H14,17), 7.80–7.79(*dd*, H15,16),	2.48-2.49(*dd*, CH_3), 4.46(b, N-H), 6.96(s H9), 7.78–7.55(*dd*, H15,16), 7.95–7.79(*dd*, H14,17), 6.03(s, H5)	2.49(*dd*, CH_3), 8.19(s, NH), 9.19(s, OH), 8.18–8.00(*dd*, H14,17), 7.99–7.55(*dd*, H15,16), 4.79(s, H9), 6.56-6.52(*dd* H3), 6.52-6.52(*dd*, H6), 6.02-6.06(*dd*, H4))	14.51(*s*, OH), 12.0(s, C=NH), 10.77(*dd*, H12), 9.49(*s*, H15), 8.77–8.56(*dd*, H16,17), 8.19(s, H8), 7.85(*dd* H3), 7.57(*dd*, H5)
	C[13]NMR	192.8(C11), 164.1(C10), 131.7-138.4(C6,8), 127.5-129.3(C2,4), 124.2(C15,16), 122.2(C12), 118.8(C13), 111.6(C9), 112.4(C14.17), 104.1(C5), 32.06 (CH_3)	183.6–181.2(C10,11), 129.5–129.2(C12,13), 126.2(C15,16), 124.5(C14,17), 116.8(C8), 108.1(C9), 168.7(C6), 141.7(C2), 132.6(C4), 119.3(C5), 23.44(CH_3)	184.5–181.5(C10,11), 134.45–133.13 (C12,13), 132.05 (C15,16), 130.65 (C14,17), 76.63 (C8), 58.26 (C9), 160.17 (C1), 158.03 (C2), 125.93 (C5), 125. 40 (C4), 110.84-110.12 (C,6), 22.31 (CH_3).	192.8(C10), 183.7 (C6), 163.9(C8), 159.2(C2), 145.9(C4), 141.4-138.4(C12,13), 131.6-129.2(C14,15), 126.4-127.5(17,18), 124.6(C11), 122.1(C3), 118.7(C16), 112.4(C5), 108.3(C9)

TABLE 3(a). CORROSION INHIBITION STUDIES AT 303K

Compounds	**Concentration**	**CR**	**% IE**	**Θ**	**∆W**
L1	BLANK	0.004	-	-	0.02
	100	0.00265	33.75	0.3375	0.01325
	300	0.00175	56.25	0.5625	0.00875
	500	0.00085	78.75	0.7875	0.00425
L2	BLANK	0.00285	-	-	0.01425
	100	0.0017	40.35	0.4035	0.0085
	300	0.00115	59.65	0.5965	0.00575
	500	0.00080	71.93	0.7193	0.004
L3	BLANK	0.0033	-	-	0.0165
	100	0.0018	45.45	0.4545	0.009
	300	0.0012	63.64	0.6364	0.006

ISSN 0795 - 22066

	500	0.00035	89.39	0.8939	0.00175
L4	BLANK	0.00205	-	-	0.01025
	100	0.00065	68.29	0.6829	0.00325
	300	0.0006	70.75	0.7075	0.003
	500	0.0005	75.61	0.7561	0.0025

Table 3(b). Corrosion Inhibition Studies at 333K

COMPOUNDS	CONCETRATION	CR	% IE	Θ	ΔW
L1	BLANK	0.01225	-	-	0.06125
	100	0.00725	40.82	0.4250	0.03625
	300	0.006125	50.00	0.5000	0.030625
	500	0.005875	52.04	0.5204	0.029375
L2	BLANK	0.01175	-	-	0.05875
	100	0.004125	64.89	0.6489	0.020625
	300	0.0015	87.23	0.8723	0.0075
	500	0.00125	88.36	0.8936	0.00625
L3	BLANK	0.012	-	-	0.06
	100	0.008375	30.21	0.3021	0.041875
	300	0.00625	47.92	0.4792	0.03125
	500	0.00575	52.08	0.5208	0.02875
L4	BLANK	0.01175	-	-	0.05875
	100	0.00775	34.04	0.3404	0.03875
	300	0.00325	72.34	0.72340	0.01625
	500	0.00275	76.60	0.7660	0.01375

Table 3(c). Corrosion Inhibition Studies at 363K

Compounds	Concentration	CR	% IE	Θ	ΔW
L1	BLANK	0.0333	-	-	0.16625
	100	0.0279	16.17	0.1617	0.13938
	300	0.0268	19.55	0.1955	0.13375
	500	0.0260	21.80	0.2180	0.13000
L2	BLANK	0.0263	-	-	0.13125
	100	0.0249	5.086	0.05086	0.12458
	300	0.0199	23.94	0.2394	0.09938
	500	0.0139	55.00	0.55	0.06938
L3	BLANK	0.0229	-	-	0.11450

ISSN 0795 - 22066

	100	0.0221	3.49	0.03493	0.11050
	300	0.0206	10.04	0.10044	0.10300
	500	0.0200	12.66	0.12664	0.10000
L4	BLANK	0.0232	-	-	0.11600
	100	0.0186	19.83	0.1983	0.09300
	300	0.0195	15.95	0.1595	0.09750
	500	0.0172	26.86	0.2686	0.08600

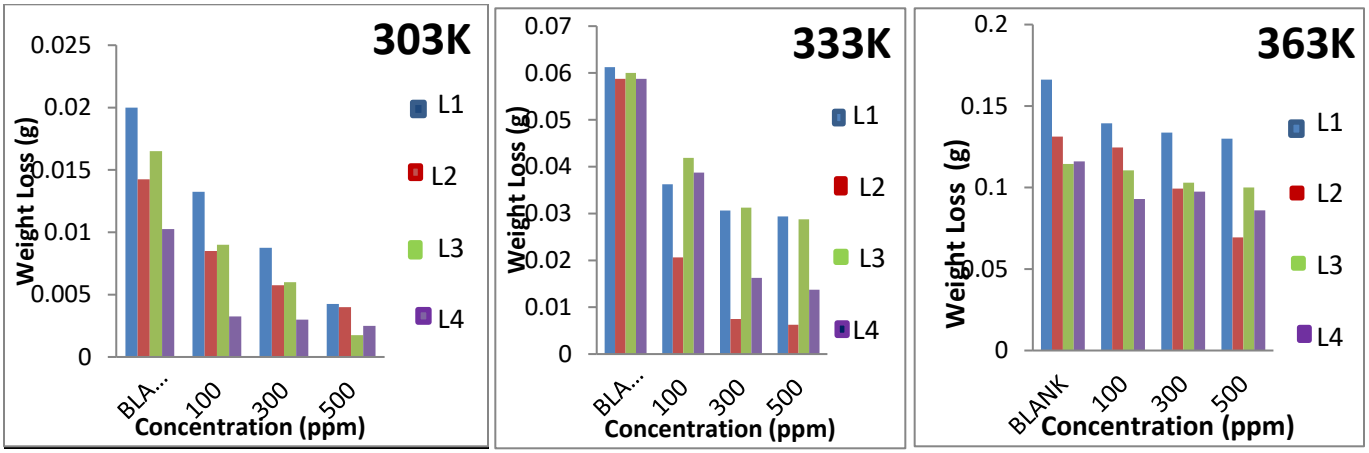

(a) (b) (c)

Figure 2: Plots of weight loss variations against concentration of inhibitors at (a) 303K (b) 333K and (c) 363K

From the graph plotted in figure 2(a), it was detected that the weight loss declined from 0.02g to 0.00425g, 0.01425g to 0.004g, 0.0165g to 0.00175g, and 0.01025g to 0.0025g for L1, L2, L3, and L4 inhibitors respectively at 303K temperature. In figure 2(b), there was a decrease in weight loss from 0.06125-0.029375g, 0.05875-0.00625g, 0.06-0.02875g, and 0.05875-0.01375g for L1, L2, L3, and L4 inhibitors respectively at 333K. Although there was an increase in weight loss at 333K temperature compared to weight loss observed at 303K temperature in figure 2(a). The increase in weight loss was as a result of increase in temperature. Finally, figure 2(c) showed similar results for L1, L2, L3 and L4 having a decrease in weight loss as concentration increased from 100 to 500ppm (0.16625-0.13000g, 0.13125-0.06938g, 0.11450-0.10000g, 0.11600-0.08600g) for L1, L2, L3 and L4 at 363K respectively. The outcome indicates an apparent drop in the weight loss owing to the acid solution. The results (Figure 2) similarly revealed that total weight loss at 363K temperature was higher compared to weight loss at 333K and 303K temperatures at constant time (5 hours). The total weight loss at all the temperatures and concentrations also established the statement that rise in concentration of the inhibitors led to reduction in CR of the ms [33].

The Effect of Inhibitor Concentration (C_{inh}) on the Rate of MS Corrosion

Figure 3(a), (b) and (c) shows the plots of CR against C_{inh} for the corrosion of ms in one mole hydrochloric acid with and without the inhibitors at diverse concentrations and constant temperature.

ISSN 0795 - 22066

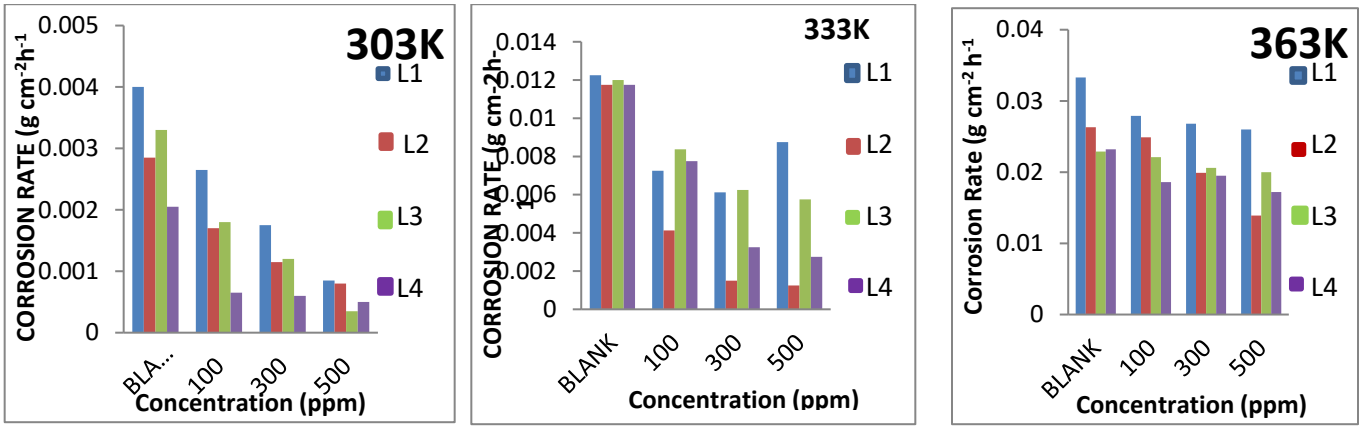

(a) (b) (c)

Figure 3. Plots of CR verse C_{inh} at different temperatures for ms corrosion in one mole hydrochloric acid in the absence and presence of the ligands

From the plots, it was detected that in the presence of the inhibitors, the CR declined in the acid solutions compared to without the inhibitors, and also decreased as the inhibition concentration increased at the same temperatures. Figures 3 (a), (b) and (c) represents plot of $\%^{\eta}wL$ versus C_{inh}. From the plots, it shows that as the concentration of the ligands increased from 100 to 500 ppm, there was increase in $\%^{\eta}wL$ at each temperature. The highest $\%^{\eta}wL$ at 303K, 333K and 363K temperatures and 500 ppm concentration were observed at 89.39% (L3), 88.36% (L2) and 55.00% (L1) respectively. The presence of heteroatoms like oxygen, sulphur and oxygen and aromatic rings with π-electrons within their structures and the capability of the heteroatoms to generate a shielding film on the surface of the corroding metal may be the reason for better inhibition performance of the ligands. The inhibition achievement of the considered ligands could be mainly as a result of the availability of heteroatoms which include; oxygen, nitrogen, sulphur and aromatic rings with π-electrons within their structures and their capacity with heteroatoms to generate a shielding film on the surface of the corroding metal [34].

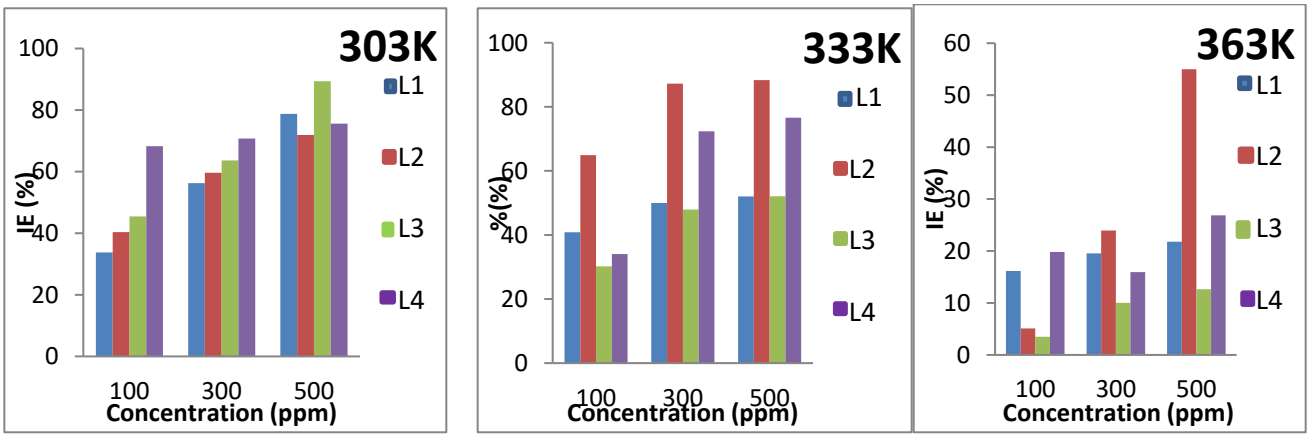

(a) (b) (C)

Figure 4. Plots of inhibition efficiencies verse C_{inh} at different temperatures for ms corrosion in 1M HCl in the absence and presence of the ligands for 5 hours

ISSN 0795 - 22066

From Table 3, a clear view shows that there was increase in percentage efficiency of inhibition with increase in inhibitor concentrations resulting to 89.39%, 78.75%, 75.61% and 71.93% at 303K temperature, 88.36%, 76.60%, 52.08%, and 52.04% at 333K temperature and 55.00%, 26.86%, 21.80% and 12.66% at 363K temperature for 5 hours immersion in 1M hydrochloric acid, for L1, L2, L3 and L4 respectively**.** This exceptional efficiency maybe accredited to the adsorption of inhibitor ligands on ms exterior surface through the free electron pairs and π-electrons of the cycle moieties together with the imine moiety. This behaviour which mirrors the inhibitive influence of the ligands against the acid corrosion of the steel, perhaps could result from adsorption of phytochemical components of the ligands on the metal surfaces. According to some literature review [8,22], increase in inhibitor concentrations results in continuous allowance in Θ as the efficacy of adsorption rises in the same manner. The order of efficiency for 5 hours immersion was L2< L4<L1<L3, L1<L3<L4<L2 and L3<L1<L4< L2 at 303K, 333K, and 363K temperature respectively with L3 having the highest %ⁿwL at 89.39% for 5 hours. Nevertheless, L2 had the least %ⁿwL of 71.93% at 303K, L1 had 52.04% at 333K and L3 had 12.66% at 363K for 5 hours respectively. The result showed that improved efficiencies of the inhibitors were dependent on the concentrations of the solution, as increase in concentration increased the efficiencies [35].

EFFECT OF TEMPERATURE

Effect of C_{inh} and Temperature on CR

The CR curves of ms in the presence and absence of ligands in one mole hydrochloric acid at different temperatures are given in figure 5. The result obtained shows that CR of ms in the medium under study, increased as the temperature increased. However, this advancement is diluted as the concentration of the ligands increases, enhancing the efficiency of the molecule as a corrosion inhibitor for ms in 1M HCl. The interpretation of this result might be as a result of formation of a film barricade that separates ms from its aggressive environment [36].

A plot of CR against temperature (Fig. 5), and relation amid CRs of ms in acidic media with temperature (T) is usually expressed by Arrhenius equation:

$$CR = A\exp\left(-\frac{Ea^{*}}{RT}\right) \text{---------- (4)}$$

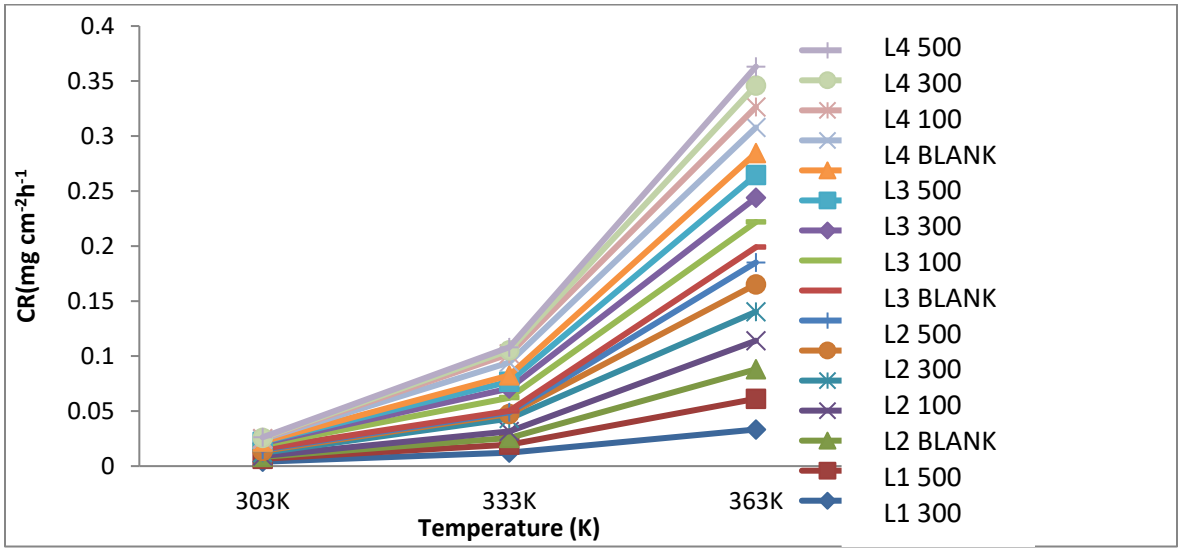

Figure 5. Progression of CR with temperature for altered concentrations of the ligands

ISSN 0795 - 22066

Table 3 reveals the progression of %ᵑwL as against temperature. The highest %ᵑwL seen was found to be 89.39%, 88.36% and 55% at 303K, 333K, and 363K for the concentration of 500 ppm. The %ᵑwL decreases when the temperature increases as shown in Table 3. This maybe as a result of effect of desorption of the inhibitor molecules [37]. Nevertheless, reduction in efficiency of the inhibitors with a rise in temperature can as well be credited to improved solubility of the shielding film and other products deposited on the metal surface. This resulted in the accessibility of the acid to corrode the metal.

Adsorption Isotherms and Thermodynamic Functions

Adsorption isotherm affords us with the basic facts on the interaction amid the ligands used as inhibitors and the metal. Langmuir adsorption isotherm was used to test this work by fitting the degree of Θ and the concentration of the inhibitor.

A plot of log CR verse 1/T (Figure 4d) gave predictable graph with -Ea/2.303R slope which helped the estimation of the activation energies (*E*a). Table 5 affirmed that *E*a of inhibitors in the inhibiting acid solution was much more than the uninhibited solutions, implying that the inhibitors inhibited the corrosion of the steel by raising the energy barrier of the corrosion reactions, and could be interpreted on the basis of physical adsorptions [38].

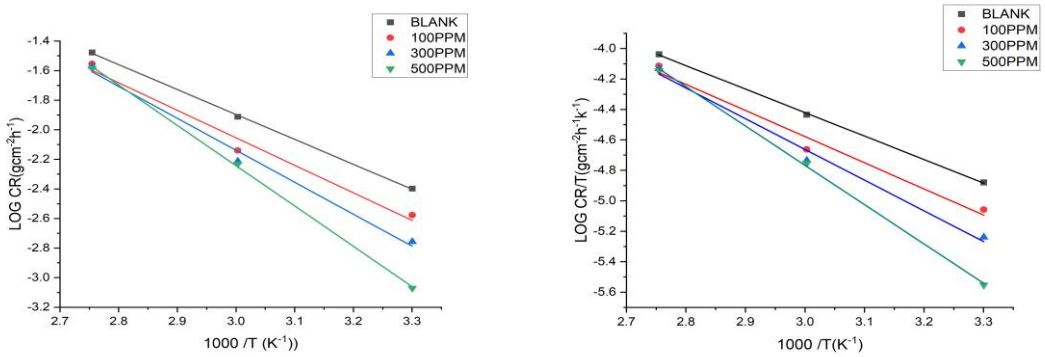

6(a) **6(b)**

Fig 6 (a) Arrhenius plots for ms corrosion in one mole hydrochloric acid in the absence and presence of L1, 6(b) Transition state plots for ms in one mole hydrochloric acid without and with various concentrations of L1

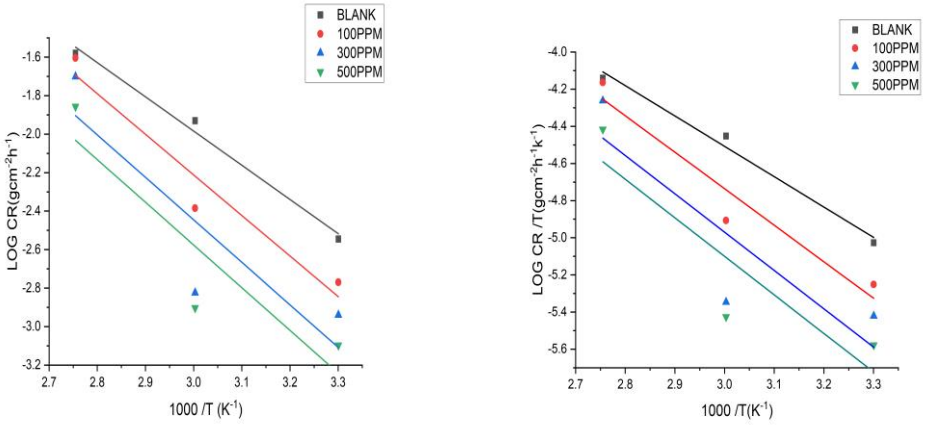

7(a) **7(b)**

Fig 7 (a) Arrhenius plots for ms corrosion in one mole hydrochloric acid in the absence and presence of L2, 7(b) Transition state plots for ms in one mole hydrochloric acid without and with various concentrations of L2

ISSN 0795 - 22066

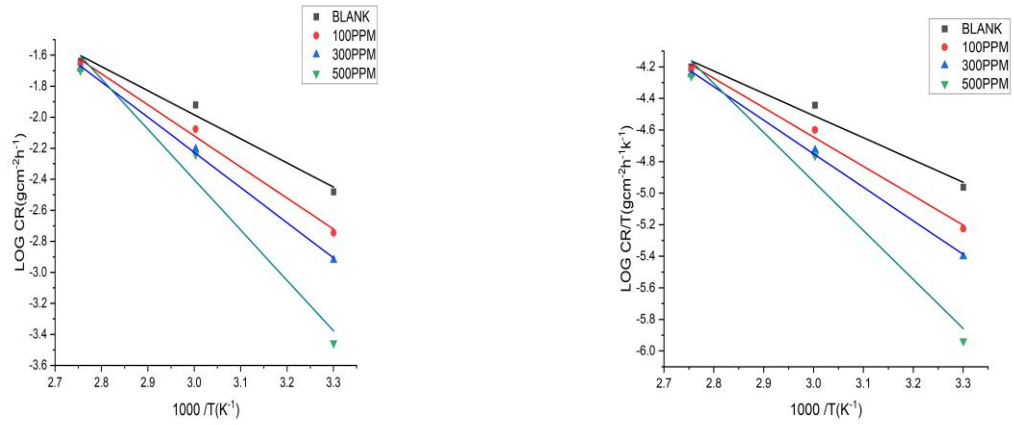

8(a) **8(b)**

Fig 8 (a) Arrhenius plots for ms corrosion in one mole hydrochloric acid in the absence and presence of L3, 8(b) Transition state plots for ms in one mole hydrochloric acid without and with various concentrations of L3

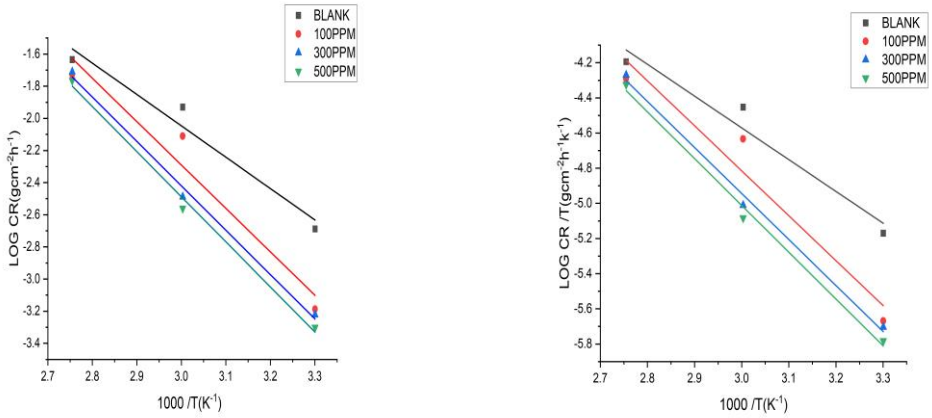

9(a) **9(b)**

Fig 9 (a) Arrhenius plots for ms corrosion in one mole hydrochloric acid in the absence and presence of L4, 9(b) Transition state plots for ms in one mole hydrochloric acid without and with various concentrations of L4

The other activation thermodynamic parameters of the corrosion reaction like enthalpy as well as entropy of activation were assessed via transition state kind of equation as presented in Table 4.

Table 4 illustrates that the value of activation, ΔH is non-negative and greater in presence of inhibitor reflecting endothermic nature of the ms dissolution process. Large and non-positive values of ΔS suggest that the activation stage of the adsorption process is controlled by associative interactions within the steel and the inhibitor molecules rather than formation of steel and H_2O molecules [39].

Adsorption Isotherm

Adsorption isotherm produce significant data about the interactions amid the inhibitor molecules and the surface of ms. The origin of adsorption isotherms that validate the adsorption of a corrosion inhibitor might give imperious traces to the behaviour of the metal-inhibitor interaction. In order to get facts regarding adsorption of ligands molecules on the mss, the Θ values derived from the gravimetric data were used to study the principal adsorption isotherm. The most repeatedly used isotherms remains: Langmuir, Temkin, Frumkin, Flory-Huggins, Bockris-Swinkels plus Dhar-Fory-Huggins. These

ISSN 0795 - 22066

adsorption isotherms (Fig 10) were tested, and among all the Langmuir isotherm affords the most outstanding fit with data of regression coefficient (R^2) near 1. Langmuir isotherm is denoted by the succeeding equation:

$$\frac{Cinh}{\theta} = \frac{1}{Kads} + c_{inh} \quad \textbf{(5)}$$

The slight nonconformities of the slopes of the Langmuir plots from harmony arose from interfaces within adsorbed molecules on the metal surface and modification in the heat of adsorption with rising Θ. The data of K_{ads} (Table 5) were acquired from the intercept ($1/K_{ads}$).

Table 4. Activation parameters for the dissolution of ms in the absence and presence of varied concentration of Ligands in one mole hydrochloric acid

LIGANDS	Concentration(ppm)	Ea(KJ mol^{-1})	ΔH(KJ mol^{-1})	ΔS(Jmol^{-1}K^{-1})
L1	BLANK	32.27426	29.5238	-193.66
	100	35.63363	32.8834	-186.6
	300	41.38463	38.6342	-170.97
	500	52.20821	49.4577	-140.49
L2	BLANK	34.06443	31.314	-189.966
	100	40.39332	37.6429	-176.343
	300	42.28518	51.0235	-174.14
	500	42.50998	39.7586	-175.969
L3	BLANK	29.74649	26.9738	-202.993
	100	38.38582	35.6352	-179.613
	300	43.43158	40.6811	-166.508
	500	62.21472	59.4643	-113.524
L4	BLANK	37.3746	34.6241	-181.233
	100	51.72299	48.9726	-142.86
	300	52.87974	50.1293	-141.867
	500	53.73164	50.981	-140.612

Table 5. Adsorption parameters determined for ligands studied as inhibitors for Ms corrosion in 1 HCl

Ligand (L)	Temperature {K}	SLOPE	K_{ads} (mg^{-1} L)	R^2	ΔG^0_{ads} (KJmol-1)
L1	303	0.84656	0.00427	0.94937	-23.8639
	333	1.81376	0.018325	0.99999	-22.1937
	363	4.18787	0.004428	0.99708	-28.4799
L2	303	1.11822	0.006826	0.99345	-22.6821
	333	1.01357	0.02064	0.99865	-21.8621
	363	2.64273	0.000461	0.96097	-35.3079
L3	303	0.84831	0.006157	0.92822	-22.9419

ISSN 0795 - 22066

	333	1.57261	0.005979	0.99872	-25.2947
	363	2.71333	0.000408	0.83444	-35.6765
L4	303	1.28713	0.040911	0.99796	-18.1709
	333	0.89742	0.00542	0.96575	-25.5665
	363	3.39304	0.002515	0.7393	-30.1873

R^2 represents the correlation coefficient, which is employed to evaluate if the adsorption model is harmonious with the methodological findings [40]. It is evident from Figures 10(a-d) that the R^2 values of the plots of concentration versus Θ were significantly different from the unit. They manifest that the ligand molecules' adsorption upon the surface of ms does not obey the Temkin isotherm. The ligands molecules adsorption upon the surface of ms follows the Langmuir adsorption. The straight lines amid (C) and (C/θ) are obtained with the correlation coefficient near to 1 (Figure 10), and the values of slope in the Langmuir formula varies between 0.84656 and 4.18787. Such outputs verify that the ligands' values upon the ms follow the Langmuir isotherm. The adsorption equilibrium constant K_{ads} falloffs with upsurge in temperature, signifying that the interfaces within the adsorbed molecules and the mss were exhausted, hence, the adsorbed molecules may become easily separable, K_{ads} is related to the standard free energy of adsorption;

$\Delta G_{ads} = -RT\ In(55.5K_{ads})$ …….(6)

The evaluated values of ΔG_{ads} for a particular temperature in presence of a variety of concentration of the ligands are likewise accessible in Table 6. The greater the K_{ad} value, the more the area of covered surface, and the more enhanced the anticorrosion film of ligands on the electrode interface. The negative data of G_{ads}^0 suggested the unprompted adsorption of ligands at the electrode/electrolyte interface [41]. The usage of ΔG_{ads} data to illustrate the approach of adsorption of inhibitor molecules on ms has been mostly conversed [41].

The negative data of ΔG_{ads} designate that the adsorption process is unprompted and the adsorbed layer on the mss is constant [42]. Values of ΔG_{ads} are repetitively used to classify adsorption technique as physiosorption (when ΔG_{ads}= -20 KJ mol^{-1} or less negative) or chemisorptions (for ΔG_{ads} = 140 KJ mol^{-1} or more negative). The ΔG_{ads} values acquired in our current research stood from -18.1709 to -35.6765KJ mol^{-1}, proposing that, the adsorption of our inhibitors on mss were physisorption.

ISSN 0795 - 22066

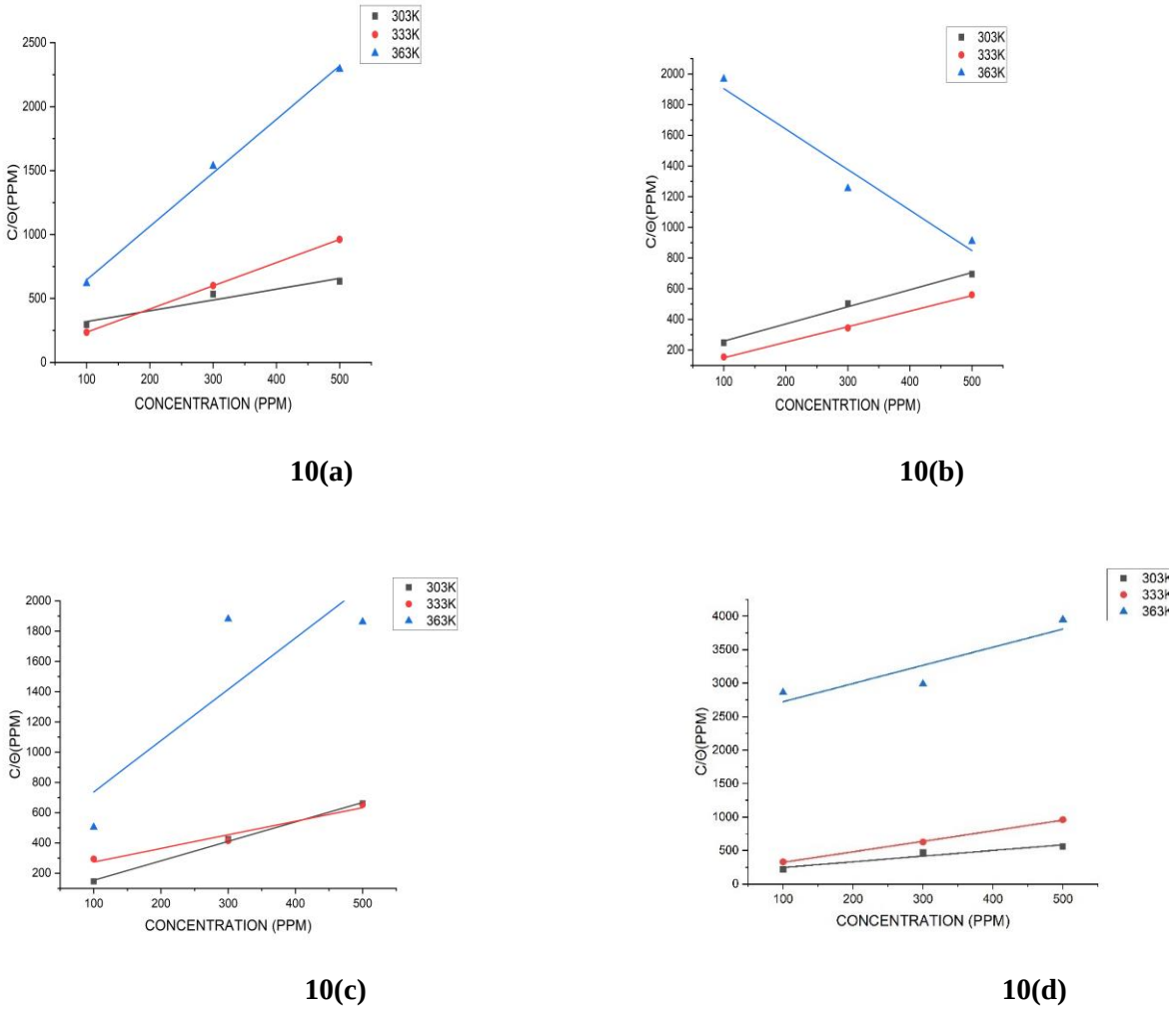

10(a) **10(b)**

10(c) **10(d)**

Figure10. Langmuir adsorption isotherms for the adsorption of ligands on the mss

Quantum (DFT) Studies

Global Reactivity

Gaussian 09 and Gauss-view variety 5.0.8 software was used to perform the quantum chemical calculations. The full optimization of considerable chemical parameters presumed for the inhibitor molecules was acquired using DFT methods [22]. Figure 11 shows the optimized chemical structure of the ligands. Figure 12 reveals the optimized HOMO and LUMO orbital structures for inhibitor molecules. The ability of an electron to be transferred arises from the interaction amid HOMO and LUMO on the basis of frontier molecular orbital (FMO) theory of chemical reactivity. An efficient corrosion inhibitor is believed to be a molecule that has large *E*HOMO and low *E*LUMO values. As revealed in Table 6, the four ligands under study have high *E*HOMO values and low *E*LUMO values. L3 has the highest *E*HOMO value (-8.4696567), followed by L2 with a value of -6.680055, L4 and L1 with least *E*HOMO value of -6.0953121 and -6.0934074 respectively. It is apparent that the HOMO level was situated on the N and O atoms; thus these positions were chosen for the electrophilic study on the metal exterior. Such explanations support the ability of the ligands to be adsorbed on the metal exterior, consequently signifying the anticorrosion ability, which agrees with the experimental outcomes [29,41]. *E*HOMO is often related with the ability of a molecule to donate electron [43]. High value of *E*HOMO compared to

ISSN 0795 - 22066

*E*LUMO, signifies that the molecule is an electron donor to a suitable electron receiver that have low empty molecular orbital. This high value enhances the adsorption which in turn inhibits corrosion on the metal surface. *E*LUMO energy shows the ability of a molecule to accept electron [43], and low values of *E*LUMO signifies that the molecule will have an enhanced potential electron acceptor. Moreover, the *E*LUMO values were -0.9705807eV for L3, -2.43910440eV for L4, -2.8192281eV for L1 and -3.1805769eV for L2. L3 has the lowest *E*LUMO than the other ligands, in agreement with experimental data. However, L3 showed greater inhibition potency than L1, L2 and L4 inhibitors.

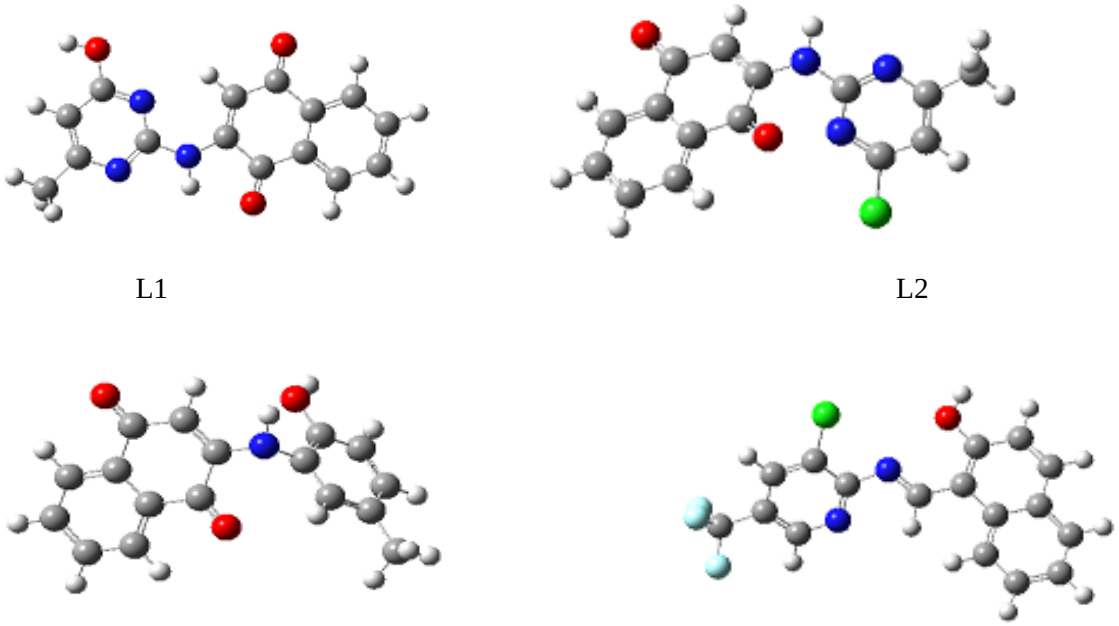

Figure 11: Optimized structures for L1, L2, L3 and L4 calculated by B3LYP/6-31G (d, p).

Table 6. Quantum Chemical Variables

Parameters/Inhibitors	L1	L2	L3	L4
E_{HOMO} (eV)	-6.0934074	-6.680055	-8.4696567	-6.0953121
E_{LUMO} (eV)	-2.8192281	-3.1805769	-0.9705807	-2.439104
Δ*E* (eV)	3.2741793	3.4994781	7.499076	3.656207
Ionisation potential (eV)	6.0934074	6.680055	8.4696567	6.0958121
Electron Affinity (eV)	2.8192281	3.185769	0.9705807	2.4391044
Electronegativity χ (eV)	4.1428442	4.93031595	4.720123185	4.2674582
Chpot	-4.1428442	-4.93031595	-4.720123185	-4.2674582
Hardness η (eV)	1.63708965	1.709987655	3.749538	1.8283538
Softness σ (eV^{-1})	0.610840096	0.584799921	0.266696536	0.54694
Electrophilicity index ω (eV)	5.241972566	7.107662738	2.970974408	4.9802198
Chemical potential μ **(**eV)	3.1658	2.0699	3.1758	5.4125

ISSN 0795 - 22066

The energy difference (ΔE) is a dynamic indicator that reveals the efficiency of inhibitors to be absorbed to the metal exterior. A low value of energy difference (ΔE) indicates a greater propensity of inhibitor to be adsorbed on the steels exterior [29, 44]. As verified in Table 6, a lesser energy gap of 3.274 eV for L1, 3.499 eV for L2, 7.499 eV for L3 and 3.656 eV for L4 indicate a transfer of electron from HOMO to LUMO. This confirms that the four ligands had good adsorption ability and increase chemical reactions as they all possess low energy gap values.

The ability of inhibitors to donate or accept an electron from the metal surface is described by electronegativity values [45]. High electronegativity values shows the capability of inhibitors to receive and take electrons from metal atoms, forming a strong bond with the metal atom [44], whereas low electronegativity values indicate the potentials of inhibitor molecules to give electrons to a metal surface. Many inhibitors demonstrate moderately low electronegativity values suggesting their capability to give electrons to a metal. From the listed data (Table 6), it is seen that the electronegativity of the four ligands were all low indicating that they were all electron donors with L2 (4.93031595eV) greater than others. Consequently, L2 established greater electron acceptance potential compared to L1(4.1428442eV), L3(4.72012185eV) and L4(4.26745825eV) [46].

A compound can be evaluated for stability and susceptibility from its η or σ values. Strong protection ability is seen with soft compounds than hard compounds because of the reliability generated by the smooth coating of electrons on the metal exterior during the adsorption, hence indicating effective shielding inhibitors [44]. The η basically signifies the opposition towards the distortion or polarity of the electron cloud of atoms, ions or molecules under small agitation of chemical reaction. A soft molecule has a small energy gap while a hard molecule has a large energy gap [47,48]. In this present work, the ligands under study had low energy gaps, therefore are soft molecule with L1 being softer than the others. The latter shows the strong ability of L1 to inhibit the donation of electrons to the observed steel, resulting in a strong anticorrosion ability.

To evaluate the exclusion value of a material, dipole moment is used [49]. Increase in dipole moment leads to increase in deformation energy and adsorption of the molecule on the studied steel. Consequently, increase in dipole moment produced an increase in the effectiveness of the corrosion inhibition [6]. Glancing through the Table 5, it was discover that L4 had a greater dipole moment value (5.4125Debye) than L1(3.1658), L2(2.0699) and L3(3.1758), which verified the tendency for L4 to be adsorbed on the steel and improve the prevention competence. However, literature researches [50] had it that many anomalies were indicated in the case of connection of μ with proficiency in inhibition. In conclusion [51], the connection between inhibition proficiencies and μ values is insignificant

The electron Affinity exposes the total energy required for a ligand to become electron acceptor while the ionization potential signifies the ability of a ligand to become an electron donor [32,41]. In this study, the result obtained for ionization potential (I) and electronic affinity (A) for L1, L2, L3, and L4 molecules reveals high values of ionization potential and low values of electron affinity representing the capacity of the molecules both to donate and accept electrons.

ISSN 0795 - 22066

The electrophilicity (ω) parameter measures the chemical reactivity because it offers information on both the hardness and chemical potential of a substance. Higher values of the ω were considered to indicate a better electrophile whereas a lower ω value reveals nucleophilic ability [41,52,53]. The low electrophilic values of Ψ = 5.2419725eV (L1), Ψ =7.10766278eV (L2), Ψ =2.970974408eV (L3) and Ψ = 4.98-21188eV (L4) molecules shows they were good nucleophile which indicates higher chemical reactivity.

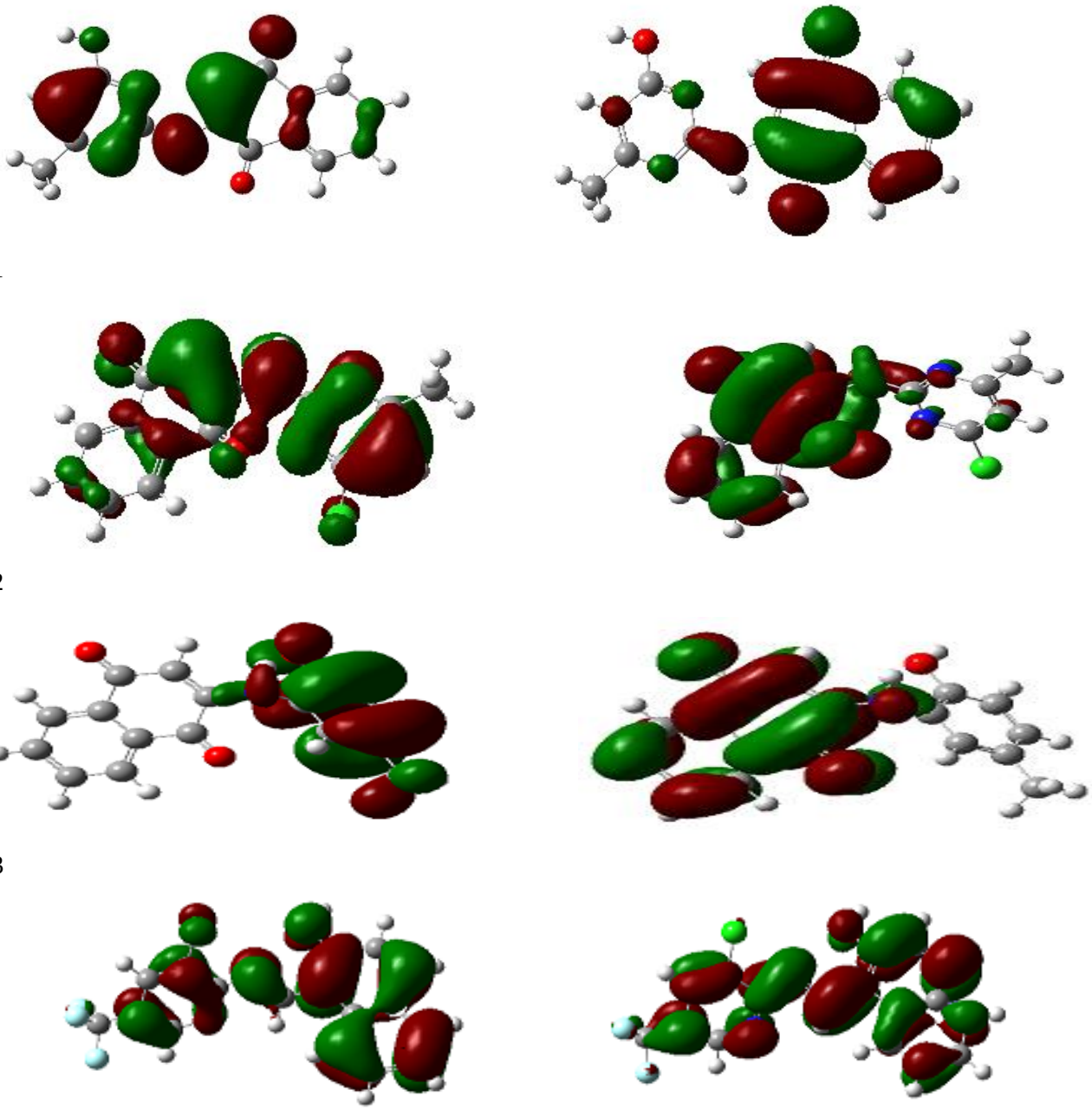

L1

L2

L3

L4 HOMO LUMO

Figure12: **HOMO and LUMO diagrams of L1, L2, L3, and L4 by B3LYP/6-31G (d, p)**

ISSN 0795 - 22066

CONCLUSION

From the experimental findings, the followings can be concluded:

- The %ηwL value rises with the concentration of the inhibitor but declines with an increase in the temperature suggesting the physical adsorption.
- This study also detected that in the presence of the inhibitors, the rate of corrosion declined compared to acid solution without ligands
- The desorption process of the four studied ligands upon the mss follows the Langmuir adsorption isotherm
- The global reactivity descriptors indicated that the 4-ligands were found to be in good agreement with both experimental and theoretical results.

REFERENCES

1. Cristofari, G., Znini, M., Majidi, L., Bouyanzer, A., Al-Deyab, S.S., Paolini, J., Hammouti, B. and Costa, J., (2011). Chemical composition and anti-corrosive activity of pulicariamauritanica essential oil against the corrosion of mild steel in 0.5M H_2SO_4. Int. J. Electrochem. Sci. 6 (2011), 6699- 6717.

2. Gupta, N.K., Verma, C., Quraishi, M.A., and Mukhrajee, A.K. (2016). Schiff's bases derived from L-lysine and aromatic aldehydes as green corrosion inhibitors for mild steel: Experimental and theoretical studies. J. of Molecular Liquids 215 (2016), 47–57. http://dx.doi.org/10.1016/j.molliq.2015.12.027.

3. Kannan, P., Karthikeyan, J., Murugan, P., Rao, T.S., and Rajendran, N. (2016). Corrosion inhibition effect of novel methylbenzimidazolium ionic liquid for carbon steel in HCl medium. J. of Molecular Liquids, 221, 368–380. doi:10.1016/j.molliq.2016.04.

4. Verma, C., Olasunkanmi, L.O., Obot, I.B., Ebenso, E.E., and Quraishi, M.A. (2016). 2,4-Diamino-5-(phenylthio)-5H-chromeno[2,3-b]pyridine3-carbonitriles as green and effective corrosion inhibitors: gravimetric, electrochemical, surface morphology and theoretical studies. RSC Advances, 6(59), 53933–53948. Doi: 10.1039/c6ra04900a.

5. Mishra, M., Tiwari, K., Singh, A.K., and Singh, V.P. (2014). Synthesis, structural and corrosion inhibition studies on Mn(II), Cu(II) and Zn(II) complexes with a Schiff base derived from 2-hydroxypropiophenone. Polyhedron, 77, 57–65. doi:10.1016/j.poly.2014.04.003

6. Singh, A., Ansari, K.R., Quraishi, M.A. and Kaya, S. (2020). Theoretically and experimentally exploring the corrosion inhibition of N80 steel by pyrazol derivatives in simulated acidizing environment. J. Mol. Struct. **2020**, 1206, 127685.

7. Anitha, C.,. Sheela, C.D., Tharmaraj, P. and Sumathi, S. (2012). Spectroscopic studies and biological evaluation of some transition metal complexes of azo Schiff-base ligand derived from (1-phenyl-2,3-dimethyl-4-aminopyrazol-5-one) and 5((4-chlorophenyl)diazenyl)-2-hydroxybenzaldehyde. Spectrochim Acta Part A: Mol. Biomol. Spectrosc., 96: 493-500.

8. Festus, C. and Wodi, C.T. (2021). Corrosion inhibition; and antimicrobial studies of bivalent complexes of 1-(((5-ethoxybenzo[d]thiazol-2-yl)Imino)methyl)naphthalene-2-ol chelator: Design, synthesis, and experimental characterizations. Direct Research J. of Chem. and Materials Science, 8(2021), 31-43. https://directresearchpublisher.org/drjcm/vol-8-november-2021/

9. Eddy, N.O., Ebenso, E.E. and Ibok, U.J. (2010) Adsorption, synergistic inhibitive effect and quantum chemical studies of ampicillin(AMP) and halides for the corrosion of mild steel in H_2SO_4. J.Appl. Electrochem, 40, 445–456

10. Zerga, B., Sfaira, M., Rais, Z., Ebn-Touhami, M., Taleb, M., Hammouti, B., Imelouane, B. and Elbachiri, A. (2009). Lavender oil as an eco-friendly inhibitor for mild steel in 1M HCl. Materiaux et Technique, 97 (2009), 297-305.

11. Umoren, S.A. Ebenso, E.E. Okafor, P.C. and Ogbobe, O. (2006). Water-soluble polymers as corrosion inhibitors. Pigment & Resin Technology, 35(6), 346–352. Doi.10.1108/03699420610711353.

12. Chioma, F. (2017). Synthesis, characterization and antibacterial studies of heteroleptic Co(II), Ni(II), Cu(II) and Zn(II) complexes of N-(2-hydroxybenzylidene)pyrazine-2-carboxamide. Int.l J. of Chem., Pharm. & Techn., 2(5); 202-211

ISSN 0795 - 22066

13. Ahmed, A.A., Abdul, A.H.K., Abu, B.M. and Sutiana, J. (2013). A novel hydrazinecarbothiamide as potential corrosion inhibitor for mild steel in HCl. Materials, 6, 1420-1431. https://doi.org/10.3390/ma6041420

14. Festus, C., Ibeji, C., and Okpareke, O. (2020a). Novel 3d divalent metallic complexes of 3-[(2-hydroxy-5-methyl-phenylimino)-methyl]-napthalen-2-ol: Synthesis, spectral characterization, antimicrobial and computational studies. J. of Molecular Structure, 1210, 128017. https://doi.org/10.1016/j.molstruc.2020.128017

15. Sankarap, S., Apavinasam, S., Pushpanaden, F. and Ahmed, M. (1991). Piperidine, piperidones and tetrahydrothiopyrones as inhibitors for the corrosion of copper in H_2SO_4. Corrosion Science, 32, 193-203.https://doi.org/10.1016/0010-938X(91)90043-O

16. Wang, L. (2001). Evaluation of 2-mercaptobenzimidazole as corrosion inhibitor for mild steel in phosphoric acid. Corrosion Science, 43, 1637-1644. https://doi.org/10.1016/S0010-938X(01)00036-1

17. Eldesoloky, A.M., Diab, M.A., El-Bindary, A.A., El-Sonbati, A.Z. and Seyam, H.A. (2015). Some antipyrine derivatives as corrosion inhibitors for copper in acidic medium: Experimental and quantum chemical molecular dynamics approach. Journal of Materials and Environmental Science, 6, 2148-2165.

18. Akpan, I.A. and Offiong, N.A.O. (2013). Inhibition of mild steel corrosion in hydrochloric acid solution by ciprofloxacin drug. Int.l J. of Corrosion, 2013, 1-5. doi.org/10.1155/2013/301689

19. Obot, I.B., Ebenso, E.E. and Kabanda, M.M. (2013). Metronidazole as an environmentally safe corrosion inhibitor for mild steel in 0.5 M HCl: Experimental and theoretical investigation. The Journal of Environmental Chemical Engineering, 1; 431-439. https://doi.org/10.1016/j.jece.2013.06.007

20. Pavithra, M.K., Venkatesha, T.V., Vathsala, K. and Nayana, K.O. (2013). Inhibiting effects of rabeprazole sulfide on the corrosion of mild steel in acidic chloride solution. Int.l J. of Electrochem., 2013, 1-9. doi.org/10.1155/2013/714372

21. Znini, M., Cristofari, G., Majidi, L., Ansari, A., Bouyanzer, A., Paolini, J., Costa, J. and Hammouti, B., (2012). Green approach to corrosion inhibition of mild steel by essential oil leaves of Asteriscus graeolens(forssk) in sulphuric acid medium. Int.l J. Electrochem. Sci. 7 (5) 3959–3981.

22. Chioma, F**.,** Ima-Bright, N. and Osi, V. (2022). Synthesis; spectral, computational studies; and antimicrobial evaluations of Fe(II) and Zn(II) chelates containing R'C-NR'' and N_2O_2 moieties. J. Anal Pharm Res. 2022; 11(2), 45–54. Doi: 10.15406/japlr.2022.11.00401.

23. Festus, C. and Don-Lawson, C.D. (2018). Synthesis, spectral, magnetic and *in-vitro* biological studies of organic ligands and their corresponding heteroleptic divalent *d*-metal complexes. The Pharmaceutical and Chemical Journal; 5(3):118-129. http://tpcj.org/archive/volume-5-issue-3-2018

24. Festus, C., Jude, I. A. and Collins, U. I. (2021). Ligation actions of 2-(3-hydroxypyridin-2-ylamino)naphthalen-1,4-dione: Synthesis, characterization, *In-vitro* antimicrobial screening, and computational studies. Indian Journal of Heterocyclic Chemistry, 31(01); 1-13.

25. Abel-Olaka, L., C., Kpee, F. and Festus, C. (2019). Solvent extraction of 3*d* metallic elements using N_2O_2 Schiff base-chelators: Synthesis and characterization. Nigerian Research Journal of Chemical Sciences. 7(2); 133-146. *http://www.unn.edu.ng/nigerian-research-journal-of-chemical-sciences/p2*

26. Haque, J., Verma, C., Srivastava, V., Quraishi, M., & Ebenso, E. (2018). Experimental and quantum chemical studies of functionalized tetrahydropyridines as corrosion inhibitors for mild steel in 1 M hydrochloric acid. *Results In Physics*, *9*, 1481-1493. https://doi.org/10.1016/j.rinp.2018.04.069

27. Chioma, F. and Theresa, W.C. (2022). Novel M^{2+} complexes of 2-(thiazol-2-ylamino)-2,3-dihydonaphthalene-1,4-dione Schiff base: Design, preparation, characterizations and corrosion inhibition studies. J. Appl. Sci., 22:152-165.

28. Festus, C., Ekennia, A.C., Osowole, A.A., Olasunkanmi, L.O. Onwudiwe, D.C. and Ujam, O.T. (2018). Synthesis, experimental and theoretical characterization and antimicrobial studies of some Fe(II), Co(II) and Ni(II) complexes of 2-(4,6-dihydroxypyrimidin-2-ylamino)naphthalene-1,4-dione. Research on Chemical Intermediates 44(10):5857-5877; DOI 10.1007/s11164-018-3460-7

ISSN 0795 - 22066

29. Festus, C., Odozi, W.N., and Olakunle, M. (2020). Preparation, spectral characterization and corrosion inhibition studies of (*e*)-*n*-{(thiophene-2-yl)methylene}pyrazine-2-carboxamide schiff base ligand. Protection of Metals and Physical Chemistry of Surfaces. 56(3), 651–662. Doi: 10.1134/S2070205120030107

30. Kpee, F., Ukachukwu, C.V. and Festus, C. (2018). Synthesis, characterization and extractive potentials of aminopyrimidine Schiff base ligands on divalent metal ions. Nigerian Research Journal of Chemical Sciences. 4(2), 193-203. https://www.unn.edu.ng/nrjcs-page2/

31. Chioma, F. and Ogechi, O. (2017). Behaviour of N-(2-hydroxybenzylidene)pyrazine-2-carboxamide in complexation towards Fe(II), Co(II), Ni(II) and Cu(II) ions: Synthesis, spectral characterization, magnetic and antimicrobial properties. International Journal of Chemistry, Pharmacy & Technology, 2(4), 143-153.

32. Odozi, W.N., Festus, C. and Muhammad, A.D. (2020). Synthesis, adsorption and inhibition behaviour of 2-[(thiophen-2-ylmethylidene)amino] pyridine-3-ol on mild steel corrosion in aggressive acidic media. Nigerian Research Journal of Chemical Sciences. 8 (2), 291-307. http://www.unn.edu.ng/nigerian-research-journal-of-chemical-sciences/ 291

33. James, A.O. and Akaranta, O. (2009). The inhibition of corrosion of Zinc in 2.0M hydrochloric acid solution with acetone extract of red onion skin. African Journal of pure and Applied Chemistry. 3(11), 212-217. https://doi.org/10.5897/AJPAC.9000165.

34. Ouedraogo, A., Diki, N.Y.S., Bohoussou, K.V., Soro, D. and Trokourey, A. (2018). Copper corrosion inhibition by cefuroxime drug in 1M nitric acid. Chemical Science Review and Letters, **7**, 427-437.

22. Silas, O., Ejiroghene, K.O. and Rogers, T., (2020). Corrosion evaluation on mild steel In different selected media. International J. of Engineering Applied Sciences and Tech., 5(3) 33-38. DOI:10.33564/IJEAST.2020.v05i03.006

35. Soroyary, N., Rayenne, D., Boulanouar, M.,Rabah, Q.(2018). Structure-corrosion inhibition performance relationship: application to some natural free acids and antioxidants. *Portugaliae Electrochimica Acta*, 36(1), 23-34

36. Diki, N.Y.S., Gbassi, K.G., Ouedraogo, A., Berté, M. and Trokourey, A. (2018). Aluminum corrosion inhibition by cefixime drug: Experimental and DFT studies. Journal of Electrochemical Science and Engineering, 8, 303-320. https://doi.org/10.5599/jese.585

37. Anbarasi, C.M. and Divya, G. (2017). A green approach to corrosion inhibition of aluminium in acid medium using Azwain seed extract. Materials Todays: Proceedings, **4**, 5190-5200. https://doi.org/10.1016/j.matpr.2017.05.026

38. Tao, Z., He, W., Wang, S., Zhang, S. and Zhou, G., (2012). A study of differential polarization curves and thermodynamic properties for mild steel in acidic solution with nitrophenyltriazole derivative. Corrostion Science, 60, 205 – 213. *https://doi.org/10.11016/j.corsci.2012.03.035*

39. Mourya, P., Singh, P., Tewari, A.K., Rastogi, R.B. and M.M. Singh, (2015). Relationship between structure and inhibition behaviour of quinolinium salts for mild steel corrosion: Experimental and theoretical approach. Corros. Sci., 95: 71-87.

40. Zinad, D.S., Salim, R.D., Betti, N., Shake, L., M. and AL-Amiery, A.A. (2022). Comparative investigations of the corrosion inhibition efficiency of a 1-phenyl2-(1-phenylethylidene)hydrazine and its analog against mild steel corrosion in hydrochloric acid solution. Prog. Color Colorants Coat. 15 (2022), 63-73

41. Gouda, M., Khalaf, M.M., Shalabi, K., Al-Omair, M.A. and El-Lateef, H.M.A. (2022). Synthesis and characterization of Zn–Organic frameworks containing chitosan as a low-cost inhibitor for sulfuric-acid-induced steel corrosion: Practical and computational Exploration. Polymers 2022, 14, 228. https://doi.org/10.3390/polym14020228.

42. Iroha, N.B. and James, A.O., (2018). Assessment of performance of velvet tamarind-furfural resin as corrosion inhibitor for mild steel in acidic solution, Journal Chem. Soc. Nigeria, 43(3), 510-517

43. Popova, A., Christov, M. and Deligeorgiev, T. (2003). Influence of the molecular structure on the inhibitor properties of benzimidazole derivatives on mild steel corrosion in 1M hydrochloric acid. Corrosion, 59, 756-764. https://doi.org/10.5006/1.3277604.

44. Abd El-Lateef, H.M., Shalabi, K. and Tantawy, A.H. (2020). Corrosion inhibition of carbon steel in hydrochloric acid solution using newly synthesized

ISSN 0795 - 22066

urea-based cationic fluorosurfactants: Experimental and computational investigations. New J. Chem. 44, 17791–17814.

45. Palaniappan, N., Cole, I.S. and Kuznetsov, A.E. (2020). Experimental and computational studies of graphene oxide covalently functionalized by octylamine: Electrochemical stability, hydrogen evolution, and corrosion inhibition of the AZ13 Mg alloy in 3.5% NaCl. RSC Adv. 10, 11426–11434

46. Upadhyay, A., Purohit, A.K., Mahakur, G., Dash, S. and Kar, P.K. Verification of corrosion inhibition of mild steel by some 4-aminoantipyrine-based Schiff bases—Impact of adsorbate substituent and cross-conjugation. J. Mol. Liq. 2021, *333*, 115960

47. Gece, G. and Bilgic, S. (2009). Quantum chemical study of some cyclic nitrogen compounds as corrosion inhibitors of steel in NaCl media. Corrosion Science, 51, 1876-1878. https://doi.org/10.1016/j.corsci.2009.04.003

48. Spirtovic-Halilovic, S., Salilovic, M., Dzudzevic-Cancar, H., Trifunovic, S., Roca, S., Softic, D. and Zavrsnik, D. (2014). DFT study and microbiology of some coumarin-based compounds containing a chalcone moiety. Journal of the Serbian chemical society 79,436-443. 102298/jsc1306280775

49. Oyebamiji, A.K. and Adeleke, B.B. (2018.). Quantum chemical studies on inhibition activities of 2,3-dihydroxypropyl-sulfanyl derivative on carbon steel in acidic media. Int. J. Corros. Scale Inhib.7, 498–508.

50. Bereket, G., Hur, E. and Ogretir, C. (2002). Quantum chemical studies on some imidazole derivatives as corrosion inhibitors for iron in acidic medium. Journal Molecular Structure: THEOCHEM, 578, 79-88. https://doi.org/10.1016/S0166-1280(01)00684-4

51. Gece, G. (2008). The use of quantum chemical methods in corrosion inhibitor studies. Corrosion Science, 50, 2981-2992. https://doi.org/10.1016/j.corsci.2008.08.043

52. Bououden, W. and Benguerba,Y. (2020). Designing, cytotoxic evaluation, molecular docking and in silico pharmacokinetic prediction of new hydrocortisone derivatives as anti asthmatics drugs. Journal of Drug Delivery and Therapeutics. 10(4), 8-16. https://doi.org/10.22270/jddt.v10i4.4128

53. Diki, N.Y.S., Coulibaly, N.H., Kambiré, O. and Trokourey, A. (2021) Experimental and theoretical investigations on copper corrosion inhibition by cefixime drug in 1M HNO_3 solution. Journal of Materials Science and Chemical Engineering, 9, 11-28.https://doi.org/10.4236/msce.2021.95002

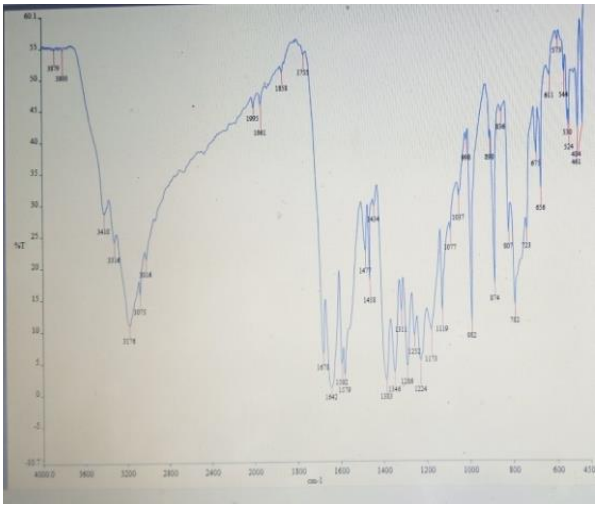

SM1. IR Spectrum of L2 Ligand

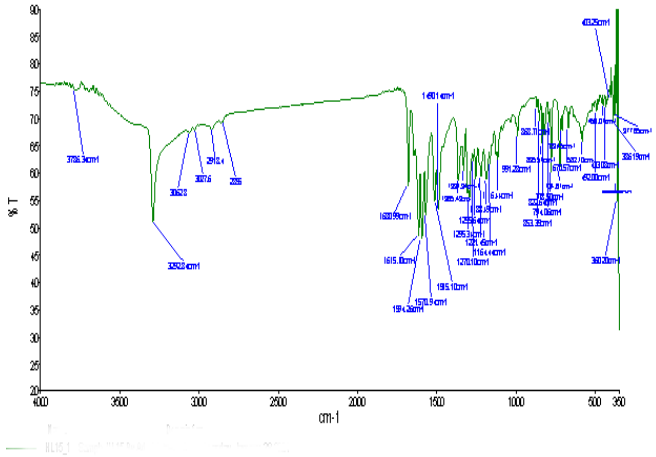

SM2. IR Spectrum of L3 Ligand

ISSN 0795 - 22066

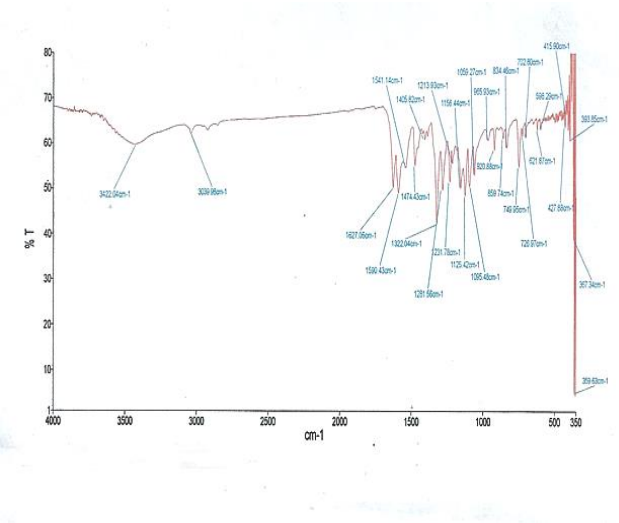

SM3. IR Spectrum of L4 Ligand

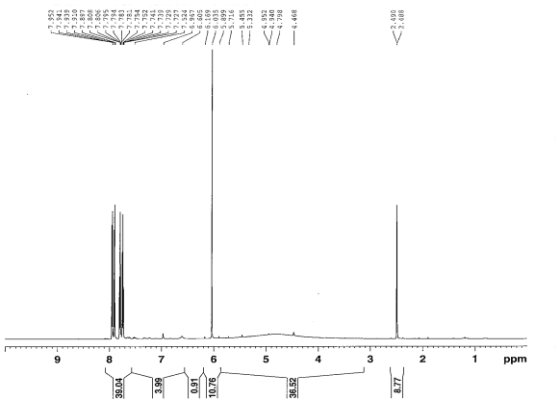

SM4. HNMR Spectrum of L2 Ligand

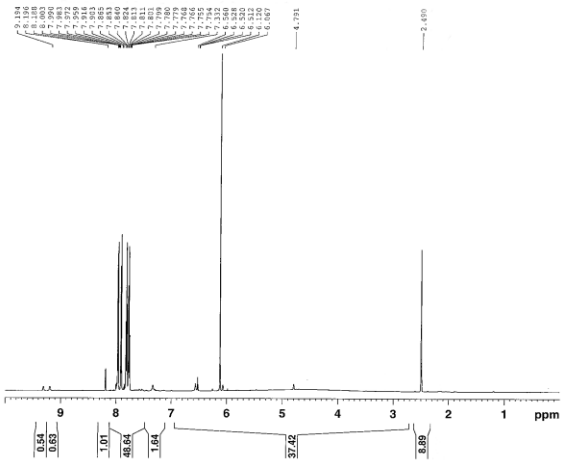

SM5. HNMR Spectrum of L3 Ligand

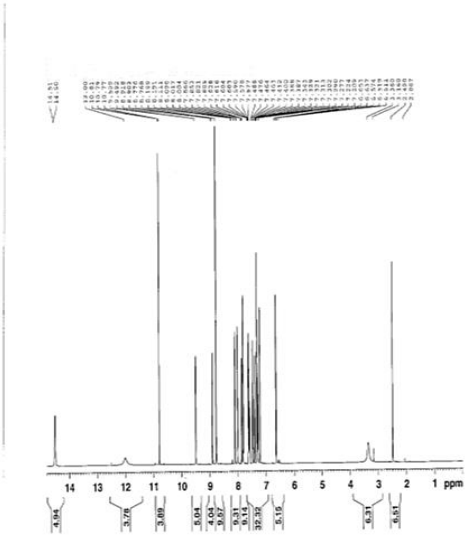

SM6. HNMR Spectrum of L4 Ligand

ISSN 0795 - 22066

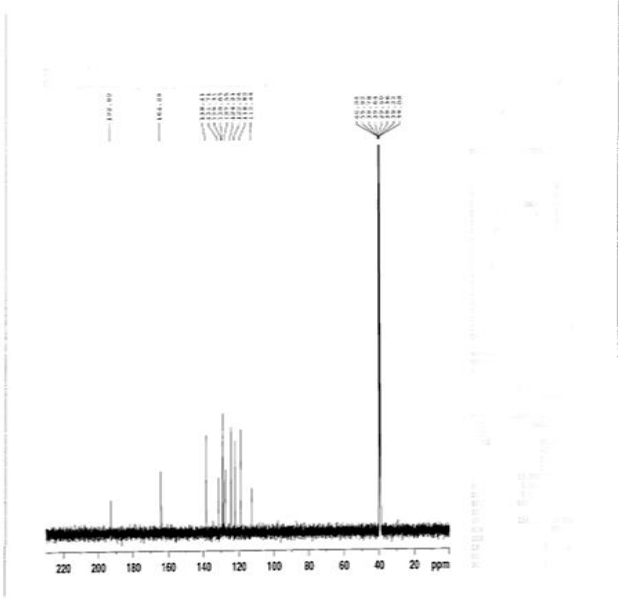

SM7. CNMR Spectrum of L1 Ligand

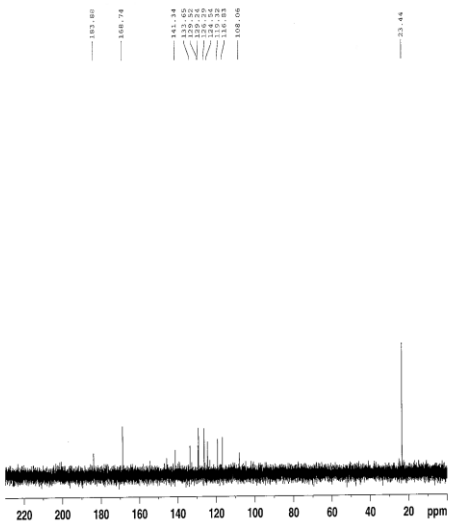

SM8. CNMR Spectrum of L2 Ligand

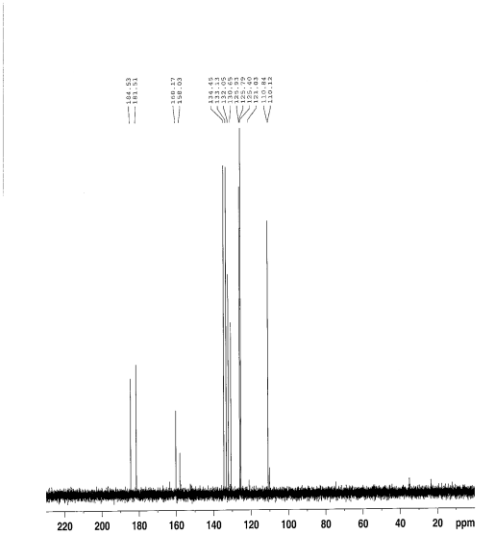

SM9. CNMR Spectrum of L3 Ligand

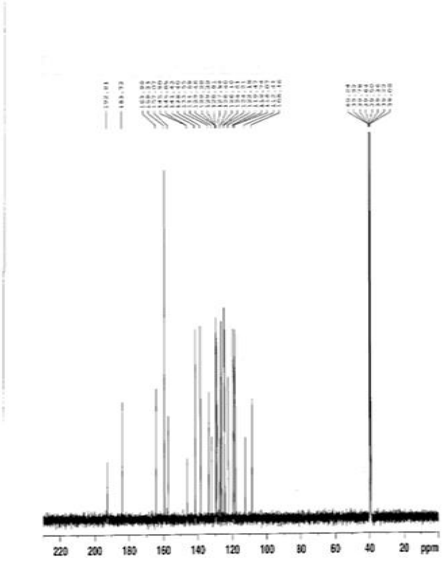

SM10. CNMR Spectrum of L4 Ligand

ISSN 0795 - 22066